Development/Plasticity/Repair

Fasciclin II Signals New Synapse Formation through Amyloid Precursor Protein and the Scaffolding Protein dX11/Mint

James Ashley,* Mary Packard,* Bulent Ataman, and Vivian Budnik
Department of Neurobiology, University of Massachusetts Medical School, Worcester, Massachusetts 01605-2324

Cell adhesion molecules (CAMs) have been universally recognized for their essential roles during synapse remodeling. However, the downstream pathways activated by CAMs have remained mostly unknown. Here, we used the *Drosophila* larval neuromuscular junction to investigate the pathways activated by Fasciclin II (FasII), a transmembrane CAM of the Ig superfamily, during synapse remodeling. We show that the ability of FasII to stimulate or to prevent synapse formation depends on the symmetry of transmembrane FasII levels in the presynaptic and postsynaptic cell and requires the presence of the fly homolog of amyloid precursor protein (APPL). In turn, APPL is regulated by direct interactions with the PDZ (postsynaptic density-95/Discs large/zona occludens-1)-containing protein dX11/Mint/Lin-10, which also regulates synapse expansion downstream of FasII. These results provide a novel mechanism by which cell adhesion molecules are regulated and provide fresh insights into the normal operation of APP during synapse development.

Key words: **Fasciclin II; amyloid precursor protein; X11; adhesion; signaling; *Drosophila*; neuromuscular junction**

Introduction

Although homophilic cell adhesion molecules (CAMs) of the Ig superfamily (IgCAMs) play critical roles in synapse plasticity (Murase and Schuman, 1999; Huntley, 2002; Packard et al., 2003; Welzl and Stork, 2003), the molecular mechanisms by which IgCAMs regulate synapse dynamics remain poorly understood (Garcia-Alonso et al., 1995; Beggs et al., 1997; Schmid et al., 1999). Mice deficient for the mammalian IgCAM neural CAM (NCAM) show impaired spatial memory as well as reduced long-term potentiation (Luthl et al., 1994; Muller et al., 1996). In *Aplysia*, long-term facilitation of the gill- and siphon-withdrawal reflex results in the formation of new synaptic connections between the presynaptic siphon-sensory neuron and the target cells. Underlying this process is the downregulation of apCAM, an *Aplysia* IgCAM, in a manner that involves mitogen-activated protein kinase (MAPK) and a ubiquitin-dependent degradation pathway (Bailey et al., 1992, 1997).

At the *Drosophila* neuromuscular junction (NMJ), as muscle fibers increase in size, synaptic efficacy is maintained by the expansion of the synaptic arbor, which continuously sprouts new synaptic boutons throughout development (Packard et al., 2003). This expansion is regulated by local changes in Fasciclin II (FasII) levels by a process that involves presynaptic activity, changes in FasII clustering, MAPK pathway-dependent FasII downregulation, and changes in FasII exocytosis (Budnik et al., 1990; Schuster et al., 1996a; Thomas et al., 1997; Koh et al., 1999, 2002; Mathew et al., 2003).

A widely accepted model posits that enhanced FasII-mediated cell adhesion constrains synaptic growth, whereas decreased FasII-mediated adhesion partially lifts this constraint, allowing for new synapses to form (Schuster et al., 1996a; Mayford and Kandel, 1999). Although this model is consistent with the observations from the above studies, it has not yet been tested fully. Indeed, almost nothing is known about the signaling mechanisms that may be activated by FasII-mediated cell adhesion. Moreover, as with other CAMs, the presence of an intracellular domain suggests that the ability of transmembrane FasII to modulate synapse formation may also involve the activation of intracellular signaling mechanisms (Biederer et al., 2002; Panicker et al., 2003).

Here, we demonstrate that FasII requires the fly homolog of amyloid precursor protein (APPL) to regulate synaptic growth and that its influence on synaptic bouton formation cannot be simply explained in terms of adhesion but by additional signaling through APPL. We show that FasII and APPL are in the same protein complex *in vivo* and that FasII–APPL signaling depends on interactions with the APPL-binding protein dX11/Mint/Lin-10/dX11L. Furthermore, we find that enhancement of new synapse formation depends on a balance of FasII levels at both sides of the synapse rather than a change in absolute levels, as suggested previously. Conversely, an imbalance of FasII levels at either side of the synapse interferes with new synapse formation and leads to gross abnormalities in bouton structure, including microtubule

Received March 23, 2005; revised May 11, 2005; accepted May 12, 2005.

This work was supported by National Institutes of Health Grant NS42629. We thank Dr. Michael Gorczyca, Dr. Hemachand Tummala, and Dennis Mathew for comments and helpful discussions on this manuscript. We also thank the Biology Microscopy Facility at the University of Massachusetts, Amherst, for support in confocal and electron microscopy and Lucy R.-S. Yin for assistance in thin sectioning for transmission electron microscopy.

*J.A. and M.P. contributed equally to this work.

Correspondence should be addressed to Vivian Budnik, Department of Neurobiology, University of Massachusetts Medical School, Aaron Lazare Medical Research Building, Seventh Floor, 364 Plantation Street, Worcester, MA 01605-2324. E-mail: vivian.budnik@umassmed.edu.

DOI:10.1523/JNEUROSCI.1144-05.2005

 0270-6474/05/255943-13$15.00/0

tangles, membranous inclusions, and abnormal APPL deposits. These studies unravel a signaling pathway activated by FasII during synapse formation and establish a link between two important modulators of synapse growth: FasII and APPL.

Materials and Methods

Fly strains. Flies were reared in standard *Drosophila* medium. The following mutant stocks were used: hypomorph $fasII^{e76}$ (Schuster et al., 1996a), null allele $Appl^{d}$ (Luo et al., 1992), double-mutant $Appl^{d}$ $fasII^{e76}$ obtained by recombination, P[UM-8095-3] (Bloomington Stock Center, Bloomington, IN), and Df(1)BK10 (Bloomington Stock Center), a deficiency of the *dX11* region. We used the following upstream activator sequence (UAS)–APPL strains [described by Torroja et al. (1999)]: UAS–$APPL^{SD}$, containing a form of APPL that cannot be proteolytically processed, UAS–APPLΔC in which the intracellular domain of APPL is deleted, and UAS–APPLΔCi, in which the cytoplasmic internalization sequence GYENPTY has been removed. We also used the following: dX11, UAS–dX11ΔPTB, in which the phosphotyrosine-binding (PTB) domain had been deleted, and the FasII UAS strain UAS–FasII–glycosylphosphatidylinositol (GPI) (see below). Gal4 activator strains used to drive motoneuron-specific expression of APPL and FasII were C164, which has Gal4 expression in type I motoneurons during larval development (Torroja et al., 1999), and C380, which has Gal4 expression in type I motoneurons (Koh et al., 1999). For expression of transgenes in body-wall muscles, we used the Gal4 drivers BG487 and C57 (Budnik et al., 1996).

Generation of transgenic flies. To generate UAS–dX11, *Drosophila* dX11 cDNA was digested with *Not*I and *Kpn*I, and the resulting insert, containing the entire *dX11* coding region, was directly cloned into pUAST vector for germline transformation (Spradling, 1986). To generate dX11 lacking the APP-binding PTB domain (dX11ΔPTB), site-directed mutagenesis was performed using the Stratagene (La Jolla, CA) QuikChange kit. Briefly, oligos were used to introduce *Xho* sites on either side of the PTB domain coding sequences (amino acids 766–986), the PTB domain was digested out, and sticky ends religated before subcloning into pUAST. To generate a UAS–GPI-linked FasII, cDNA LP01422 was digested with *Eco*RI and ligated into the pUAST vector.

Immunocytochemistry and antibody production. Immunocytochemistry and laser-scanning confocal image acquisition and analysis were as performed by Budnik et al. (1996) using a Bio-Rad (Hercules, CA) MRC600 or a Zeiss (Oberkochen, Germany) LSM confocal microscope and Zeiss PASCAL 3.0 software. To quantify synapse number, third instar body-wall muscle preparations were labeled with a neuronal marker (anti-HRP, which cross-reacts with several presynaptic membrane antigens, thus labeling the entire presynaptic arbor), and boutons were counted at muscles 6 and 7 of abdominal segment 3. To quantify the number of buds, the following criteria were used to identify buds: (1) buds were much smaller than the parent boutons, and (2) they appeared to sprout from a neighboring "parent" bouton of mature bouton size. To measure muscle surface, the width and length of muscles 6 and 7 were measured under epifluorescence using a calibrated ocular grid. For the expression of FasII, dX11, or APPL variants using the UAS/Gal4 system (Brand and Perrimon, 1993), crosses and rearing of larvae were performed at 29°C to maximize levels of Gal4 expression. Controls at this temperature were also performed for wild-type, homozygous Gal4 strains, homozygous UAS–APPL strains, and Gal4/UAS–*LacZ* heterozygotes. No significant differences in bouton number were observed in these controls. The number of buds and boutons was expressed (mean ± SEM) and compared using the Student's *t* test. To quantify APPL levels inside a bouton, a single confocal slice at the bouton midline was selected, and APPL fluorescence intensity in the ring of HRP staining at the bouton membrane (APPLm) was measured. APPL fluorescence at the internal region of the bouton (APPLi), the area circumscribed by the ring of HRP staining, was then added to the intensity value by using the histogram function of the Zeiss LSM software. Then background intensity, obtained by measuring APPL fluorescence intensity in surrounding muscle, was subtracted, after normalizing the intensity measurements to surface area. Numbers were expressed as percentage of total APPL fluorescence (normalized APPLi/normalized APPLm plus APPLi). The following antibodies were used to label synaptic terminals: FITC- or Texas Red-conjugated anti-HRP (1:200), anti-FasII (1:3500) (Koh et al., 1999), anti-APPL952 (1:500) (Torroja et al., 1996), anti-dX11 (1:100; see below), anti-tubulin (1:1000; Sigma, St. Louis, MO), and monoclonal antibody 22C10 (1:100; a gift from S. Benzer, Developmental Studies Hybridoma Bank, University of Iowa, Iowa City, IA. Secondary antibodies (Jackson ImmunoResearch, West Grove, PA) were used at 1:200.

Anti-dX11 antibodies were generated by immunizing rats and rabbits with bacterially generated and affinity-purified His-tagged protein (dX11 N-terminal amino acids 137–266), produced using the pET System (Novagen, Madison, WI). The rabbit antiserum was subsequently affinity purified (Tang, 1993).

Immunoprecipitations. For immunoprecipitations, 20–40 body-wall muscle preparations per genotype were homogenized at 4°C in radioimmunoprecipitation assay (RIPA) buffer containing protease inhibitors and 100 μm Na_3VO_4. After centrifugation (3000 × *g* for 5 min), the supernatant was precleared with Protein A- or Protein A/G-agarose beads for 1 h. Cleared lysate was subsequently incubated with beads bound to rat anti-dX11 or rabbit anti-APPL952 at 4°C for 1–2 h and then washed three times with PBS. Beads and the bound immunocomplexes were then collected by centrifugation, washed three times with RIPA buffer, and boiled in loading buffer. Proteins were separated in an 8% SDS-PAGE gel, transferred to Immobilon-P (Millipore, Billerica, MA) nylon membrane, and sequentially blotted with rabbit anti-APPL952 (1:1000), rat anti-dX11N1 (1:1000), mouse anti-tubulin (1:5000; Sigma), and rabbit anti-FasII (1:1000).

Schneider cell transfection. dX11 and fasII cDNAs were cloned into the pAcV5/HisB vector (Invitrogen, Carlsbad, CA) for transfections. *Drosophila* Schneider (S2) cells were cultured in HYQ SFX-Insect cell culture medium (HyClone, Logan, UT) containing 10% FBS, penicillin (100 U/μl), and streptomycin (100 μg/μl). Three wells (2 ml each) per sample of 60–80% confluent S2 cells were transfected with 1.5 μg of DNA using Cellfectin (Invitrogen). Thirty-six hours after transfection, cells were harvested, resuspended in 300 μl of RIPA buffer, and homogenized, and immunoprecipitations were performed as described above for body-wall muscles. For RNA interference (RNAi) experiments, dX11 double-stranded RNA (dsRNA) was generated using dX11 primers containing a 5′T7 polymerase-binding site and applied to S2 cells, as described by Clemens et al. (2000).

Electron microscopy. Ultrastructural analysis was as performed by Jia et al. (1993), with the exception of the use of 2 mM Mg^{2+} Trump's fixative (Torroja et al., 1999). Transverse ultrathin serial sections (70–80 nm) were cut from ventral longitudinal muscles 6 and 7 at abdominal segments A3 and A4. Three wild-type (10 boutons), three [FasII, APPL]-pre (12 boutons), and three [FasII]-pre (eight boutons) samples were used for this analysis.

Electrophysiology. All experiments were performed on wandering third instar larvae raised at 29°C. Larvae were dissected under ice-cold hemolymph-like (HL-3) saline (Stewart et al., 1994) containing 0.3 mM calcium. Body-wall muscles were visualized under a Zeiss Axiovert 200 using a 40× long-working distance objective and continually superfused with HL-3 saline containing 0.5 mM calcium at 22°C. Recordings were done by impaling body-wall muscle 6 in abdominal segment 3 with a 15–20 MÙ electrode and were amplified using an Axoclamp 2A amplifier (Molecular Devices, Union City, CA). Recordings were exported to both an ITC-16 computer interface (InstruTech, Port Washington, NY) and a Neuro-Corder (Neurodata Instruments, New York, NY) for data storage. Data were imported via Pulse software (HEKA Electronik, Lambrecht/Pfalz, Germany) and analyzed using both Mini Analysis software (Synaptosoft, Decatur, GA) and Origin software (OriginLab, Northampton, MA). Evoked excitatory junctional potentials (EJPs) were induced through application of a 10-μm-diameter lumen glass-suction electrode to a cut segmental nerve and stimulated with a 1 ms suprathreshold stimulus at 1 Hz by an S48 stimulator and an SIU-5 stimulus isolation unit (Grass-Telefactor, West Warwick, RI). Only muscle cells with a resting potential of −60 to −63 mV were used for analysis, and at least five cells were analyzed for each genotype. Statistical analysis was performed using the Student's *t* test.

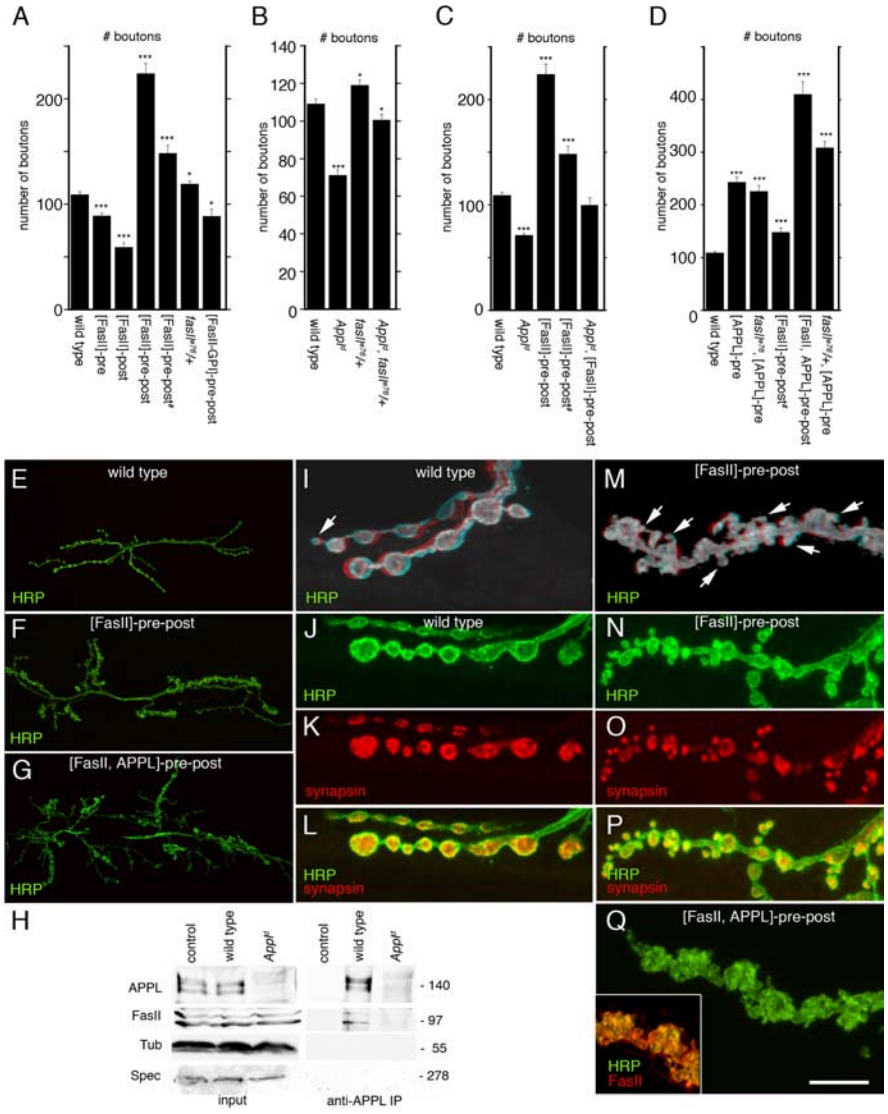

Figure 1. FasII signaling through APPL stimulates NMJ growth, and both proteins form a complex *in vivo*. ***A–D***, Histograms showing the number of boutons at muscles 6 and 7 (abdominal segment 3) of third instar larvae with different levels of FasII and APPL. The number of samples quantified is as follows: wild type, $n = 95$; $fasII^{e76}/+$, $n = 12$; [FasII]-pre, $n = 43$; [FasII]-post, $n = 17$; [FasII]-pre-post (using the Gal4 drivers C380 and BG487), $n = 13$; [FasII]-pre-post$^{\#}$ (using the Gal4 drivers C164 and C57), $n = 10$; $Appl^{d}$, $n = 49$; [APPL]-pre (using Gal4 driver C380), $n = 14$; [APPL]-pre* (using the Gal4 driver C164), $n = 85$; $Appl^{d}$, $fasII^{e76}/Appl^{d}$, $+$, $n = 24$; $Appl^{d}$, [FasII]-pre-post (using the Gal4 drivers C164 and C57), $n = 10$; [GPI–FasII]-pre-post (using the Gal4 drivers C380 and BG487), $n = 6$; [FasII, APPL]-pre-post$^{\#}$ (using the Gal4 drivers C380 and BG487), $n = 27$; [FasII, APPL]-pre, $n = 25$; [FasII, APPLΔC]-pre, $n = 10$; $fasII^{e76}$, [APPL]-pre, $n = 21$. Bouton numbers are mean values ± SEM. $*p < 0.05$; $***p < 0.0001$. Low- (***E–G***) and high- (***I–Q***) magnification views of third instar larval NMJs at muscles 6 and 7 stained with anti-HRP (***E–G***, ***I***, ***J***, ***L–N***, ***P***, ***Q***), the synaptic vesicle marker anti-synapsin (***K***, ***L***, ***O***, ***P***), and anti-HRP and anti-FasII (***Q***, inset). ***E***, ***I–L***, Wild type. ***F***, ***M–P***, Larvae overexpressing only FasII in both presynaptic and postsynaptic cells. ***G***, ***Q***, Larvae overexpressing both APPL and FasII in both presynaptic and postsynaptic cells. ***I***, ***M***, Stereoscopic images showing budding boutons in wild type (***I***) and [FasII]-pre-post (***M***). Note the dramatic increase in budding boutons in larvae overexpressing FasII either alone or in combination with APPL. Scale bars: (in ***Q***) ***E–G***, 50 μm; ***I–Q***, 8 μm. ***H***, FasII and APPL coimmunoprecipitate from body-wall muscle extracts. Extracts were immunoprecipitated with anti-APPL antibodies, and immunoblots were sequentially probed using anti-APPL, anti-FasII, anti-tubulin (Tub), and anti-spectrin (Spec). Input lanes correspond to 10% of the extract used for immunoprecipitation. Control lanes correspond to extracts in which antibody was omitted during immunoprecipitation. Note that anti-APPL immunoprecipitates FasII and that this interaction is specific because no FasII band could be detected in $Appl^{d}$. Molecular weights are indicated in kilodaltons to the right of each blot. Error bars represent SEM.

Results

Does FasII constrain synaptic growth?

Previous studies of NMJ expansion have suggested a basic model of FasII function at the NMJ, in which enhanced FasII-mediated cell adhesion constrains synaptic growth, whereas decreased FasII-mediated cell adhesion partially lifts this constraint, allowing for new synapses to form (Schuster et al., 1996a,b). In those studies, FasII levels were decreased by using hypomorphic *fasII* alleles as well as mutations that decrease FasII expression at the NMJ, which resulted in greater synaptic growth. However, the consequences on synaptic bouton number of enhancing FasII expression either presynaptically or postsynaptically, or both simultaneously, was not examined in those studies. In subsequent work, Davis et al. (1997) examined the effects of changing FasII levels in the stabilization of ectopic innervation. The main finding in this study was that increasing FasII in specific muscles during the embryonic period led to the stabilization of inappropriate synaptic connections, but no such effect was observed when FasII levels were altered in the postembryonic period, when most synaptic boutons are formed (Davis et al., 1997).

To further explore the above hypothesis, we labeled NMJs at the last stage of larval development with a presynaptic terminal marker (anti-HRP; see Materials and Methods), and the degree of NMJ expansion was determined by counting the number of synaptic boutons (Budnik et al., 1990; Gorczyca et al., 1993). In agreement with the basic model, overexpression of FasII either presynaptically or postsynaptically resulted in a significant decrease in bouton number (Fig. 1*A*). Surprisingly, however, and in contrast to the above model, we found that when FasII levels were simultaneously elevated in both the presynaptic and postsynaptic cells ([FasII]-pre-post), there was a remarkable increase to >150–230% of the number of synaptic boutons compared with wild type, depending on the strength of the Gal4 drivers used to express UAS–FasII (Fig. 1*A*). When FasII was simultaneously decreased in both the presynaptic and postsynaptic cells in $fasII^{e76}/+$ heterozygotes, the result was a small but significant increase in bouton number, as seen in the studies of Schuster et al. (1996) (Fig. 1*A*). These changes in bouton number (and in all of the mutants examined in Fig. 1) were not attributable to changes in muscle size, which was indistinguishable from wild-type controls. Also, because we used Gal4 drivers that drive expression of transgenes during the postembryonic period, no ectopic synapses were observed. Therefore, changes in bouton number were not the result of defects in targeting and stabilization of ectopic synapses, which occur after changing FasII levels during initial embryonic synaptogenesis (Davis et al., 1997). Thus, a simultaneous decrease or a simultaneous increase in FasII levels in both the presynaptic and the

postsynaptic cells results in an increase in bouton number, albeit to different extents.

An important distinction to be made, however, is that the striking increase in bouton number that we observed in [FasII]-pre-post was primarily attributable to proliferation of "satellite" boutons or buds. In the wild type, NMJs expand in part by sprouting or budding new boutons (Fig. 1*I*, arrow), commonly at the distal end of a branch (Zito et al., 1999; Packard et al., 2002; Ruiz-Canada et al., 2004). These buds enlarge and then separate from the parent bouton, remaining connected only by a thin process, and eventually grow to become mature boutons. In NMJs overexpressing FasII in both presynaptic and postsynaptic cells, the dramatic increase in satellites/buds, 672% over wild type, was observed at both distal and proximal boutons (Fig. 1*M–P*, arrows in *M*). In contrast, satellite number in $fasII^{e76}$/+ decreased to 33% of the wild-type value [8.6 ± 1.1 in wild type ($n = 30$) vs 74.5 ± 5.22 in [FasII]-pre-post ($n = 9$) and 2.8 ± 0.6 in $fasII^{e76}$/+ ($n = 12$)]. To determine whether the buds observed in [FasII]-pre-post represented an enhancement of the normal process of bouton budding observed in wild type, we performed an ultrastructural analysis of buds. We found that buds in [FasII]-pre-post were similar to those observed in wild type, including the distribution of synaptic vesicles, active zones, and postsynaptic specializations (supplemental Fig. 1, available at www.jneurosci.org as supplemental material).

The above observations suggest that the influence of FasII on synaptic growth may not be purely related to its "adhesive" properties that are proposed to restrict synapse expansion, but may also involve the activation of a signaling cascade that promotes bud formation. This signaling cascade might depend on homophilic binding between FasII molecules at the presynaptic and postsynaptic cell, because overproliferation of boutons was observed only after changing FasII levels in both the presynaptic and the postsynaptic cells (Fig. 1*A* and below).

Transmembrane FasII isoforms can form dimers through homophilic interactions that require their extracellular Ig domains, but FasII also contains a 136 aa intracellular domain (Grenningloh et al., 1991), which may transduce a signal to the intracellular milieu. To determine whether the increase in bouton number in [FasII]-pre-post depended on an intact intracellular domain, we generated transgenic flies carrying the GPI-linked FasII isoform (GPI–FasII), in which the intracellular and transmembrane domains are missing, and expressed it presynaptically and postsynaptically. No increase in bouton number was observed in [GPI–FasII]-pre-post, demonstrating that the effect of FasII on bouton number depended on an intact intracellular domain (Fig. 1*A*).

FasII requires APPL to modulate synaptic bouton formation

The spectacular increase in bouton buds observed at NMJs overexpressing FasII at both presynaptic and postsynaptic cells was highly reminiscent of the phenotype observed in NMJs with increased APPL (Torroja et al., 1999), a presynaptically localized homolog of APP. Overexpressing APPL in motoneurons results in an increase in bouton number to >250% of wild type, primarily because of an overproliferation of bouton buds, but also because of a proliferation of mature boutons, whereas a null mutation in *Appl*, $Appl^{d}$, reduces bouton number (Torroja et al., 1999) (Fig. 1*B*,*D*).

The similarity of the results between overexpression of FasII and APPL raised the possibility that FasII may activate APPL-dependent mechanisms that promote synaptic growth. We tested this possibility by looking for genetic and biochemical interactions between APPL and FasII. In these experiments, we modified the levels of both proteins by generating both loss- and gain-of-function double mutants. As noted, a reduction in FasII levels in $fasII^{e76}$/+ resulted in a small but significant increase in bouton number (Fig. 1*B*). This increase in bouton number was completely suppressed in an *Appl* null mutant background ($Appl^{d}$, $fasII^{e76}/Appl^{d}$, +), and furthermore, the number of synaptic boutons actually decreased compared with wild type in this double mutant (Fig. 1*B*). These data lend support to the notion that *Appl* and *fasII* genes interact and that the increase in bouton number observed in $fasII^{e76}$/+ may result from interactions with APPL.

This hypothesis was further tested by simultaneously overexpressing FasII in both the presynaptic and postsynaptic cells in the *Appl* null mutants ($Appl^{d}$, [FasII]-pre-post). Again, we found that in the absence of APPL, overexpressing FasII in both the presynaptic and the postsynaptic cell led to a wild-type number of boutons, in contrast to the twofold increase when APPL levels were normal (Fig. 1*C*).

Another phenotype elicited by a symmetric increase or decrease in FasII was a rise in the number of NMJ branches (supplemental Fig. 2*A*, available at www.jneurosci.org as supplemental material). Again, as in the case of bouton overproliferation, this phenotype was completely suppressed by the absence of APPL (supplemental Fig. 2*A*, available at www.jneurosci.org as supplemental material).

To determine whether APPL was acting downstream of FasII, we performed the converse experiment, by determining whether a severe reduction in FasII function in $fasII^{e76}$ homozygotes could rescue the bouton overproliferation observed by increasing APPL levels. However, we found that a decrease in FasII levels in the presence of elevated APPL ($fasII^{e76}$, [APPL]-pre) did not rescue the increased bouton number observed in APPL gain-of-function alone (Fig. 1*D*). Thus, the increase in bouton number observed when there is a simultaneous increase or decrease in presynaptic and postsynaptic FasII levels requires the presence of APPL, indicating that APPL exerts its effects downstream of FasII during synaptic bouton growth.

This hypothesis was further confirmed by experiments in which APPL expression was upregulated in larvae in which FasII was simultaneously enhanced in both the presynaptic and the postsynaptic cell ([FasII, APPL]-pre-post). In this case, the increase in bouton number was further potentiated to >400% (Fig. 1*D*,*G*,*Q*). Together, the results from the above genetic approach uncover a novel transduction pathway by which FasII regulates synapse structure and function through interactions with APPL.

A potential association of FasII and APPL into an endogenous protein complex was examined by immunoprecipitation assays using body-wall muscle extracts. We found that antibodies against APPL coimmunoprecipitated FasII from body-wall muscle extracts, but this was not observed in extracts from *Appl* null mutants, demonstrating the specificity of the immunoprecipitation (Fig. 1*H*). Furthermore, spectrin, which is particularly enriched at synaptic boutons (Ruiz-Canada et al., 2004) was not coprecipitated by APPL antibodies, demonstrating selectivity for the complex (Fig. 1*H*). Thus FasII and APPL interact genetically during NMJ expansion and are present in a biochemical complex *in vivo*.

Functional consequences of altering FasII and APPL levels

Although APPL has been shown previously to be involved in the regulation of synaptic bouton formation (Torroja et al., 1999), the functional consequences of altering APPL levels have not been investigated. Similarly, the functional consequences of in-

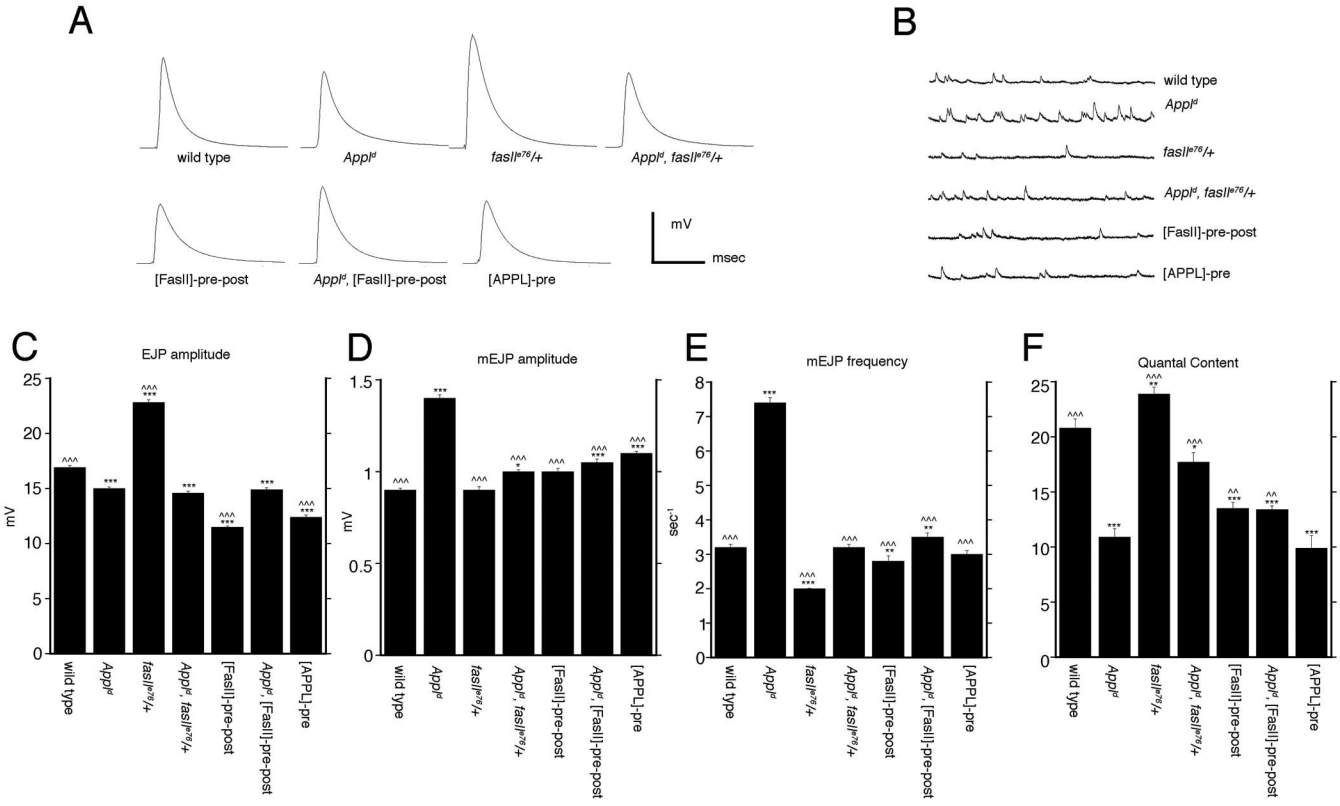

Figure 2. Electrophysiological analysis of APPL and FasII genetic variants. ***A***, Representative traces of evoked EJPs, in which each trace is the average of 400 EJPs, in wild-type; *Appl*^{d}; *fasII*^{e76}/+; *Appl*^{d}, *fasII*^{e76}/+; [FasII]-pre-post; *Appl*^{d}, [FasII]-pre-post; and [APPL]-pre. ***B***, Representative mEJP traces of the same genotypes shown in ***A***. ***C–F***, Histograms showing mean ± SEM of evoked EJP amplitude (***C***), mEJP amplitude (***D***), mEJP frequency (***E***), and quantal content (***F***). A single asterisk indicates significance in relation to wild type; triple carets or triple asterisks indicate $p < 0.0001$; double carets or double asterisks indicate $p < 0.05$. Calibration: ***A***, 10 mV, 20 ms; ***B***, 7 mV, 100 ms. Error bars represent SEM.

creasing bouton number by symmetric changes in FasII in *fasII*^{e76}/+ and [FasII]-pre-post are not known (but see Schuster et al., 1996b). Therefore, we recorded intracellularly from body-wall muscles and stimulated segmental nerves to visualize EJPs. In *fasII*^{e76}/+ animals, EJPs had significantly larger amplitudes than wild-type controls ($p < 0.0001$) (Fig. 2*A*,*C*), possibly reflecting the increased number of mature boutons in these mutants. In contrast, EJP amplitude in *Appl* null mutants was significantly decreased ($p < 0.0001$), albeit to a smaller extent (Fig. 2*A*,*C*). This phenotype may also reflect the decrease in bouton number observed in this mutant. In agreement with our hypothesis that many of the synaptic functions of FasII may occur through interactions with APPL, the increased EJP amplitude in *fasII*^{e76}/+ was completely suppressed in the absence of APPL in *Appl*^{d}, *fasII*^{e76}/+, and furthermore, it was indistinguishable from *Appl*^{d} mutants (Fig. 2*A*,*C*).

Unexpectedly, when FasII was expressed both presynaptically and postsynaptically, EJP amplitude was significantly decreased compared with both wild type and *Appl*^{d} (Fig. 2*A*,*C*). This may reflect the fact that much of the synaptic bouton overproliferation in [FasII]-pre-post is attributable to the formation of immature boutons or buds. In agreement with this view, overexpressing APPL, which also causes an overproliferation of buds, also leads to a decrease in EJP amplitude (Fig. 2*A*,*C*). As in the case of *fasII*^{e76}/+, the [FasII]-pre-post phenotype was completely suppressed by the absence of APPL, and again, EJP amplitudes were indistinguishable from *Appl*^{d} (Fig. 2*A*,*C*). This result demonstrates that defects in the postsynaptic signal derived from altering FasII levels depend on APPL.

To determine whether the defects in EJP amplitude were likely to be derived from changes in either presynaptic or postsynaptic function, or both, we also examined the amplitude and frequency of miniature EJPs. Although changes in mEJP amplitude are often attributable to changes in postsynaptic function, changes in mEJP frequency are associated with changes in presynaptic function. Furthermore, *Drosophila* larval NMJs can display compensatory mechanisms that may in certain instances adjust presynaptic and postsynaptic responses to maintain synaptic efficacy (Stewart et al., 1996; Davis and Goodman, 1998; Paradis et al., 2001). We found that, in *Appl*^{d}, mEJP frequency and mEJP amplitude were dramatically increased (Fig. 2*B*,*D–F*), perhaps as a consequence of such a compensatory mechanism. Overall, however, junctional quantal content (QC = EJP amplitude/mEJP amplitude), a measure of synaptic efficacy, was still significantly depressed (Fig. 2*F*).

In *fasII*^{e76}/+ mutants, mEJP amplitude was unchanged, and mEJP frequency was significantly decreased. However, QC was significantly enhanced (Fig. 2*B*,*D–F*). This rise in QC was suppressed by *Appl*^{d}, again suggesting that APPL is required for at least some of the functional pathways regulated by FasII. Indeed, changes in QC in [FasII]-pre-post were not rescued by the absence of APPL (Fig. 2*B*,*D–F*). Thus, although all of the structural and many of the functional defects associated with changes in FasII levels depend on APPL, these results also suggest that changes in FasII can alter NMJ function independently of APPL.

Asymmetric changes in FasII expression interfere with normal synapse development

In contrast to observations in which symmetric changes in FasII at both the presynaptic and the postsynaptic cell resulted in an

increase in bouton number, we found that a grossly asymmetric change in FasII levels brought about by overexpressing FasII in either the presynaptic or the postsynaptic cell alone interfered with normal NMJ expansion. When FasII was increased only in the presynaptic or the postsynaptic cell, there was a significant decrease in bouton number (Fig. 1*A*). Furthermore, an asymmetric increase in FasII levels in the presynaptic cell partially suppressed the increase in bouton number observed in the APPL gain-of-function alone ([FasII, APPL]-pre) (supplemental Fig. 2*B*, available at www.jneurosci.org as supplemental material). These results, together with the observation that increasing FasII levels decreases bouton number in an asymmetric manner in either the presynaptic or postsynaptic cells, suggest that an imbalance in FasII expression in both cells acts in a dominant-negative manner that interferes with the ability of APPL to promote synapse formation or that inhibits APPL activation by FasII.

This view was supported by the observation that synapses were dramatically altered not only in number but also in structure when FasII was asymmetrically expressed. This was particularly evident when FasII was expressed presynaptically in the APPL gain-of-function but was also observed in the presence of normal APPL (see below). In wild type, type I boutons at muscles 6 and 7 consist of strings of boutons, which are relatively homogeneous in size, and are joined by short neuronal processes (Johansen et al., 1989). In the [FasII, APPL]-pre gain-of-function double mutants, many type I boutons were strikingly enlarged compared with controls (Fig. 3*A*, *B*,*D*,*H*, arrows in *B*). In addition, these NMJs were characterized by very long neuritic processes, which were devoid of boutons for long stretches (Fig. 3*B*, arrowheads). These "giant" boutons contained internal membranous structures that stained brightly with the neuronal membrane marker anti-HRP (Fig. 3*D*,*H*), and which contained unusual APPL (Fig. 3, compare *E*, *I* with *F*, *J*; *L*, arrows) and FasII (Fig. 3, compare *M*, *P* with *N*, *Q*) protein accumulation.

The above phenotype was not simply attributable to overexpressing APPL and FasII at nonphysiologically high levels, because symmetrically overexpressing FasII in both the presynaptic and the postsynaptic cell in the presence of increased levels of APPL ([FasII, APPL]-pre-post) did not result in this phenotype at the NMJ. However, to further eliminate this possibility, we expressed APPLΔC, a form of APPL lacking a domain that is required for the synapse-promoting function of APPL (Torroja et al., 1999). We found that overexpressing FasII in the presynaptic cells together with APPLΔC ([FasII, APPLΔC]-pre) did not result in the formation of abnormal synaptic boutons (Fig. 3*C*) or in APPL (Fig. 3*G*,*K*) and FasII (Fig. 3*O*,*R*) deposits. Thus, the phenotypes observed in [FasII, APPL]-pre are specific and depend on an intact APPL cytoplasmic domain.

The phenotypes observed in [FasII, APPL]-pre larvae were also present, although to a much lesser extent, in boutons overexpressing only FasII in the presynaptic cell alone in the presence of normal (endogenous) APPL ([FasII]-pre). These boutons had internal structures that stained with anti-HRP and that were associated with abnormal accumulations of APPL (not shown). These inclusions were virtually never observed in wild-type boutons.

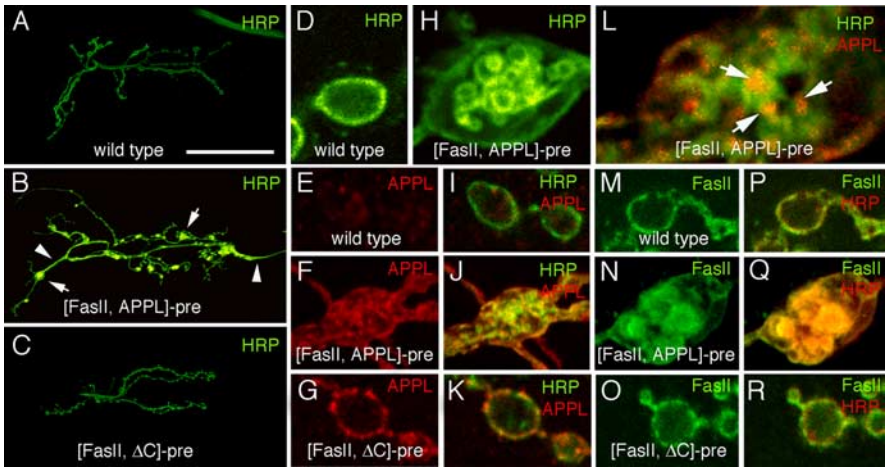

Figure 3. Gross asymmetric changes in FasII levels interfere with APPL-mediated synaptic growth. ***A–C***, Low-magnification views of third instar larval NMJs at muscles 6 and 7 stained with anti-HRP antibodies in wild type (***A***), a mutant presynaptically overexpressing both APPL and FasII (***B***), and a larva expressing FasII and APPLΔC presynaptically (***C***). ***B***, Note the dramatically enlarged boutons in the [FasII, APPL]-pre (arrows) and the long stretches of neuritic processes lacking varicosities (arrowheads). ***D–R***, High-magnification single confocal slices through a bouton in wild type (***D***, ***E***, ***I***, ***M***, ***P***), [FasII, APPL]-pre (***H***, ***L***, ***F***, ***J***, ***N***, ***Q***), and [FasII, APPLΔC]-pre (***G***, ***K***, ***O***, ***R***). Note the internal inclusions and abnormal APPL accumulations in mutants expressing both FasII and APPL and the lack of inclusions and APPL accumulations in samples in which a form of APPL lacking the cytoplasmic domain (ΔC) is expressed. ***L***, Image at higher magnification shows anti-APPL accumulations (arrows) in a [FasII, APPL]-pre bouton. ***M–R***, High-magnification single confocal sections showing anti-FasII (***M–O***) and anti-HRP and anti-FasII (***P–R***) in wild type (***M***, ***P***), [FasII, APPL]-pre (***N***, ***Q***), and [FasII, APPLΔC]-pre (***O***, ***R***). Note that the internal FasII-positive inclusions in boutons expressing both APPL and FasII only presynaptically is suppressed when the APPL cytoplasmic domain is absent, demonstrating the specificity of the interaction between APPL and FasII. Scale bars: (in ***A***) ***A–C***, 50 μm; ***I***, 3 μm; ***D–K***, ***M–R***, 5 μm.

Formation of microtubule tangles and APPL deposits in giant boutons

In Alzheimer's disease, neurofibrillary tangles are composed of cytoskeletal components including an unusual hyperphosphorylated form of the microtubule-associated protein tau (Spillantini and Goedert, 1998; Selkoe and Podlisny, 2002). Hyperphosphorylated tau is unable to promote or maintain microtubule stability because, unlike normal tau, this form is unable to bind to microtubules (Iqbal et al., 1998). The result is the formation of collections of tangled cytoskeletal filaments throughout the cytoplasm of neurons in patients with Alzheimer's disease and other disorders associated with senile dementia. Although alterations in APP processing have been widely accepted as playing a key role in Alzheimer's pathology, no clear mechanistic connection has yet been made between APP and tangle formation. At the fly NMJ presynaptic microtubules are associated with the microtubule-associated protein 1B-related protein Futsch (Hummel et al., 2000; Roos et al., 2000). Futsch immunoreactivity, as determined by the monoclonal antibody 22C10, colocalizes with presynaptic microtubules at wild-type NMJs and is observed as a single filamentous bundle that traverses the center of each NMJ branch (Fig. 4*A–C*). At certain boutons, often located at the distal end of an NMJ branch (terminal boutons), microtubules become unbundled, and their association with Futsch is lost (Ruiz-Canada et al., 2004). We found that, in enlarged [FasII, APPL]-pre boutons, even when the giant bouton was not at the end of a branch, Futsch appeared defasciculated into multiple filaments that spread inside the giant boutons (Fig. 4*E–G*, arrow in *F*), or formed large clusters or puncta inside these giant boutons (Fig.

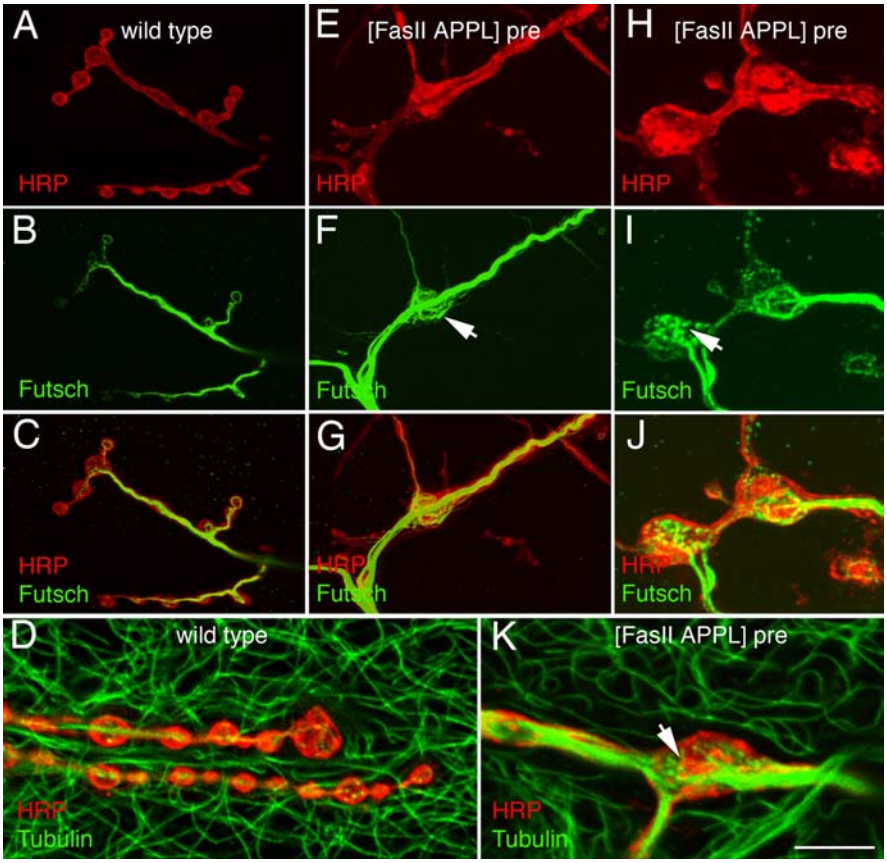

Figure 4. Microtubule tangles and abnormal APPL deposits are observed at NMJs of [FasII, APPL]-pre larvae. ***A–C***, ***E–J***, NMJs from wild type (***A–C***) and larvae overexpressing presynaptic FasII and APPL (***E–J***) showing anti-Futsch (***B***, ***C***, ***F***, ***G***, ***I***, ***J***), anti-HRP (***A***, ***C***, ***E***, ***G***, ***H***, ***J***), and merged panels (***C***, ***G***, ***J***). ***D***, ***K***, Anti-HRP and anti-tubulin in wild type (***D***) and [FasII, APPL]-pre (***K***). Note the disorganized appearance of Futsch and microtubules in mutant NMJs (***K***, arrow). Scale bar: (in ***K***) ***A–C***, ***E–J***, 10 μm; ***D***, ***K***, 6.5 μm.

4*H–J*, arrow in *I*). The distribution of microtubules, as determined by staining with antibodies against tubulin, was also greatly disrupted inside these boutons. In the [FasII, APPL]-pre larvae, unlike wild type, presynaptic microtubules were found forming defasciculated tangles that filled the boutons and often surrounded the APPL-filled internal membrane structures (Fig. 4*D*,*K*). As an internal control, postsynaptic microtubules in the muscle cells were normal in [FasII, APPL]-pre larvae (Fig. 4*D*,*K*).

To understand the structural basis for the above phenotypes ultrastructural studies were conducted. Wild-type boutons are bound by a presynaptic membrane, which surrounds the synaptic vesicles, mitochondria, and endosomes (Fig. 5*A*). In contrast, the giant boutons were characterized by the presence of many internal membranes, sometimes arranged into concentric layers (Fig. 5*C*). Some of the compartments defined by these internal membranes contained synaptic vesicles and mitochondria. However, active zone T-bars were only observed at the outer perimeter of these giant boutons (Fig. 5*C*, arrows).

Another abnormal phenotype observed in [FasII, APPL]-pre gain-of-function mutants was the presence of an unusually large number of coated vesicles in both the presynaptic and the postsynaptic compartments (Fig. 5*B*,*D*, arrowheads). Altogether, these results suggest that asymmetric changes in FasII levels interfere with APPL-dependent stimulation of synapse growth, and demonstrate a formation of unusual internal membranous and cytoskeletal tangles, in which APPL aberrantly accumulates.

The stimulation of bouton budding by FasII and APPL depends on the cytosolic adaptor protein dX11

The above results are consistent with a FasII signaling mechanism that depends on APPL. Our previous studies have demonstrated that the ability of APPL to enhance synaptic bouton number depends on its cytoplasmic domain (Torroja et al., 1999). Overexpressing APPL results in a large increase in bouton buds. This proliferation of buds is completely suppressed when an APPL variant lacking the entire cytoplasmic region is expressed. Furthermore, expressing an APPL variant (APPLΔCi), in which an amino acid sequence is deleted at the cytoplasmic region (GYENPTY), suppresses the overproliferation of buds. These observations have led to the suggestion that the GYENPTY sequence is fundamental for the regulation of bud number (Torroja et al., 1999).

In mammals, the GYENPTY sequence is conserved and is required for endocytosis of APP (Lai et al., 1998; Perez et al., 1999). Proteins that bind to the GYENPTY sequence modulate APP trafficking and/or prevent the cleavage of APP at the cell surface (Borg et al., 1996; Sastre et al., 1998; Sabo et al., 1999; Ando et al., 2001; Taru et al., 2002; King et al., 2003). One such protein is X11/Mint, which is highly expressed in neurons (King and Turner, 2004). X11 contains two postsynaptic density-95/Discs large (DLG)/zona occludens-1 (PDZ) domains and one phosphotyrosine interaction/PTB domain that interacts with APP (Zhang et al., 1997). Yeast two-hybrid assays and studies in heterologous cells show that APP and X11 interact and that deleting the PTB domain prevents these interactions (Borg et al., 1996; Zhang et al., 1997; Sastre et al., 1998; Tomita et al., 1999). Similarly, in flies, it has been demonstrated that APPL and the *Drosophila* homolog of X11, dX11/dX11L, interact *in vitro* and in a yeast two-hybrid assay (Hase et al., 2002). However, the ability of the proteins to interact in an *in vivo* context has not been tested.

To determine whether dX11 and APPL interact *in vivo* and whether dX11 might be involved in the FasII–APPL signaling cascade that leads to new synaptic bouton formation, we generated polyclonal antibodies against the N-terminal amino acids 136–266 of dX11 for use in immunocytochemistry. Controls for the specificity of this antibody included Western blot analyses of body-wall muscles and S2 cell extracts showing that anti-dX11 recognized a band of the appropriate molecular weight, dsRNAi in S2 cells, which eliminated immunoreactivity in Western blots, and overexpression of transgenic dX11, which increased immunoreactivity levels in tissue and Western blots (see below).

At wild-type NMJs, we found that dX11 was localized in puncta at presynaptic boutons (Fig. 6*A–E*). Therefore, we performed immunoprecipitations with anti-dX11 antibodies to determine whether APPL exists in a complex with dX11 and FasII at the body-wall muscles (Fig. 7*A*). Consistent with this notion, in wild-type body-wall muscle extracts, immunoprecipitation with dX11 antibodies coprecipitated endogenous APPL and FasII but

failed to coprecipitate tubulin or spectrin, demonstrating the specificity of the immunoprecipitation (Fig. 7*A*). When APPL levels were enhanced using UAS–APPL, the levels of APPL, but not of FasII, were also enhanced in the dX11 immunoprecipitation. This suggested that FasII may be included in the complex because of its interactions with dX11 and not with APPL. This possibility was addressed by performing the immunoprecipitations in the absence of APPL, in the *Appl* null mutant, as well as from larvae expressing an APPL variant lacking the GYENPTY sequence, the known site of interaction between dX11 and APPL. We found that, in both situations, the coprecipitation of FasII by dX11 was substantially increased, suggesting that dX11 can interact with FasII independent from APPL (Fig. 7*A*). Furthermore, because the coprecipitation between FasII and dX11 is stronger in the absence of APPL, these results suggest that APPL may negatively regulate the binding between dX11 and FasII. We also confirmed that the interaction between APPL and dX11 depended on the PTB domain *in vivo*, as suggested previously by using the yeast two-hybrid assay (Hase et al., 2002) (Fig. 7*B*).

The above results suggest that FasII can interact *in vivo* with dX11 in the absence of APPL. However, the possibility exists that FasII and APPL can additionally interact independently of dX11. Because no *dX11* null mutant is currently available (but see below), this possibility was addressed by transfecting *Drosophila* S2 cells. S2 cells express endogenous APPL and dX11 but virtually no FasII (Fig. 7*C*, input). However, we found that endogenous dX11 could be completely eliminated by using dsRNA (Fig. 7*C*, input). To address the possibility that APPL and FasII may interact with independence from dX11, we transfected S2 cells with dX11 and FasII. In some of these experiments, S2 cells were additionally treated with dX11 dsRNA to eliminate endogenous dX11. We found that antibodies against APPL strongly coprecipitated both FasII and dX11 in cells double transfected with FasII and dX11, and no such coprecipitation was observed in untransfected cells (Fig. 7*C*). However, similar levels of FasII were coprecipitated by APPL antibodies when cells were treated with dX11 dsRNA, despite the dramatic reduction in dX11 levels in treated cells (Fig. 7*C*). Because substantial residual dX11 was still detected in the extracts despite dX11 dsRNA treatment, we repeated these experiments in cells transfected with only FasII, with the expectation that dsRNA would completely eliminate endogenous dX11. We found that, in this case, dX11 dsRNA completely eliminated endogenous dX11, but FasII was still coprecipitated (Fig. 7*C*). These results suggest that APPL and FasII can also interact even in the absence of dX11.

These observations show that dX11 is present at the NMJ and that it interacts with both APPL and FasII *in vivo* and in S2 cells. To understand the significance of dX11 during NMJ expansion, we used several approaches, including the characterization of a hypomorphic *dX11* mutant, the generation of transgenic flies carrying full-length dX11 (UAS–dX11) to be used for gain-of-function studies, and the generation of flies carrying a *dX11* transgene lacking the APPL-binding PTB domain (UAS–dX11ΔPTB). In our coprecipitation experiments, we found that the dX11ΔPTB transgene reduced the interactions between dX11 and APPL (Fig. 7*B*). For the loss-of-function studies, we used a strain carrying a P-element insertion 169 bp from the *dX11* gene transcription start ($dX11^{P}$). Western blot analysis of body-wall muscles from $dX11^{P}$ over a deficiency of the *dX11* region, Df(1)BK10, demonstrated that, in this mutant, there was a substantial decrease in dX11 signal, but the levels of FasII and APPL were normal (Fig. 7*D*).

Notably, we found that overexpression of dX11 in motoneurons resulted in a substantial increase in bouton number [Figs. 6*G–I* (arrowheads in *H*), 7*E*,*F*]. Like NMJs overexpressing FasII presynaptically and postsynaptically, and overexpressing APPL presynaptically, the increase in bouton number was primarily attributable to an enhanced proliferation of buds (Fig. 6*H*, arrowheads). The opposite phenotype, a decrease in bouton number, was observed in $dX11^{P}/Df$ mutants (Fig. 7*E*,*F*). This phenotype is similar in extent to $Appl^{d}$ mutants. In both transgenic larvae and mutants, however, the size of the muscles was signifi-

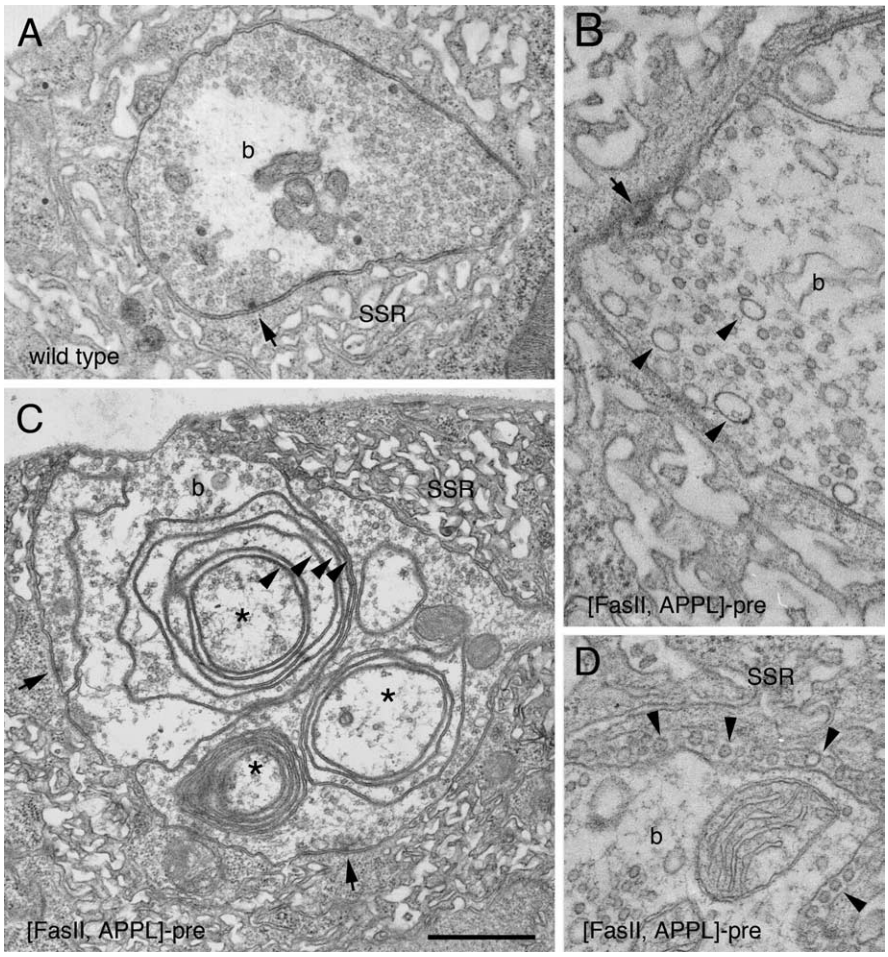

Figure 5. Electron microscopy of abnormal bouton structure in [FasII, APPL]-pre mutants. ***A–D***, Midline cross-sections through wild type (***A***) and [FasII, APPL]-pre (***B–D***) boutons. Note the presence of three groups of abnormal concentric rings (***C***, asterisks) of internal membranes (***C***, arrowheads) in the mutant, the numerous presynaptic coated vesicles (***B***, arrowheads), and the large number of postsynaptic vesicle-like structures (***D***, arrowheads). b, Bouton; SSR, subsynaptic reticulum; arrows point to presynaptic densities. Scale bar: (in ***C***) ***A***, ***C***, 0.8 μm; ***B***, ***D***, 0.4 μm.

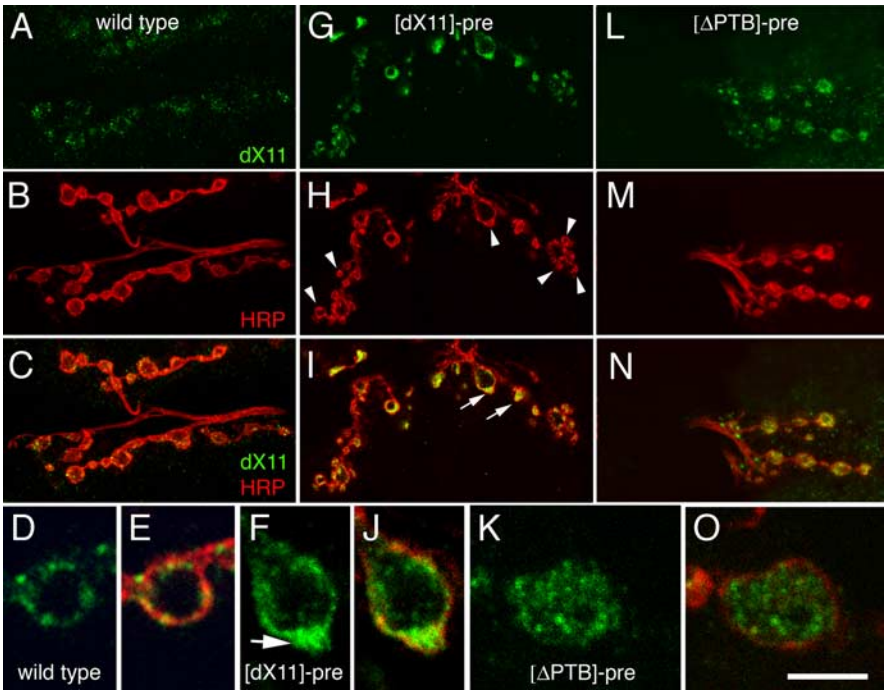

Figure 6. dX11 and APPL are found in a complex at the NMJ, and changes in dX11 levels mimic changes in APPL levels. ***A–C***, ***G–I***, ***L–N***, Single confocal slices of NMJs stained with anti-dX11 (***A***, ***G***, ***L***), anti-HRP (***B***, ***H***, ***M***), and merged panels (***C***, ***I***, ***N***). ***A–O***, Specimens are wild type (***A–E***), larvae overexpressing dX11 presynaptically ([dX11]-pre; ***F–J***), and larvae expressing a dX11 variant missing the PTB domain ([ΔPTB]-pre; ***K–O***). ***D–F***, ***J–K***, ***O***, High-magnification views of boutons from the above genotypes, showing the localization of dX11 in each case. Note that, in wild type and [dX11]-pre, dX11 staining is enriched at the presynaptic membrane (***E***, ***J***), but only in [dX11]-pre does the protein accumulate at sites of budding (***F***, arrow). ***K***, In contrast, in dX11ΔPTB, dX11 immunoreactivity is observed within the bouton cytoplasm. ***I***, ***F***, Arrows point to buds accumulating dX11. ***H***, Arrowheads point to buds. Scale bar: (in ***O***) ***A–C***, ***G–I***, ***L–N***, 12 μm; ***D–F***, ***J–K***, ***O***, 3 μm.

cantly different from control. Therefore, for the quantification of boutons, numbers were normalized by the muscle surface area (Fig. 7*F*). To determine whether the increase in boutons in [dX11]-pre depended on the presence of APPL, we expressed dX11 in the *Appl* null mutant background. We found that the increase in bouton number observed by dX11 overexpression was not affected by the lack of APPL in $Appl^{d}$ null mutant larvae, suggesting that dX11 acts downstream of APPL (Fig. 7*E*,*F*). Moreover, after presynaptic expression of dX11ΔPTB, which cannot interact with APPL, overproliferation of buds was not observed, and NMJs were either indistinguishable from wild-type controls or had a significant increase in the number of mature boutons depending on the strength of the UAS–dX11ΔPTB used (Fig. 7*E*,*F*). Furthermore, expressing dX11ΔPTB completely suppressed the increase in budding observed in [FasII]-pre-post (Fig. 6*L–N*), demonstrating that dX11 acts downstream of FasII [8.6 ± 1.1 buds in wild type ($n = 30$); 25.2 ± 2.3 buds in [dX11]-pre ($n = 14$); 0.8 ± 1.4 buds in [dX11ΔPTB]-pre ($n = 10$); 1.25 ± 0.33 in $dX11^{P}/Df$ ($n = 16$); 7.8 ± 1.6 buds in [FasII, dX11ΔPTB]-pre-post ($n = 6$)]. Thus, FasII requires both APPL and dX11 to stimulate bouton budding.

Interestingly, in [dX11]-pre, the highest levels of dX11 immunoreactivity were observed in developing buds, which appeared as protrusions at the edge of parent boutons (Fig. 6*I*,*F*, arrows, *J*). Conversely, in the case of presynaptic expression of dX11ΔPTB, no enrichment of dX11 was found at the presynaptic membrane, and rather dX11ΔPTB became abnormally localized within the bouton cytoplasm (Fig. 6*K*,*O*).

The distribution of APPL was also altered in dX11ΔPTB and $dX11^{P}/Df$ (Fig. 8). In wild type, APPL is found at very low levels at the NMJ associated with the bouton membrane and within the bouton cytoplasm (Torroja et al., 1999) (Fig. 8*A*,*B*). Although anti-APPL immunoreactivity is low at NMJs of wild type, this signal is highly specific, because it is completely suppressed in *Appl* null mutants (Torroja et al., 1999). In $dX11^{P}$/Df mutants, there was an increase in the levels of APPL inside the boutons, and APPL often appeared there in large accumulations (Fig. 8*F*,*G*,*J*,*K*) (supplemental Fig. 2*C*, available at www.jneurosci.org as supplemental material). This was even more evident in NMJs expressing the dX11ΔPTB construct, which resulted in strong APPL accumulations inside all boutons (Fig. 8*R–S*). In contrast, boutons had normal FasII localization in all dX11 genotypes (Fig. 8*C*,*D*,*H*,*I*,*L*,*M*,*P*,*Q*,*T*,*U*).

Discussion

Here, we demonstrate that the ability of FasII to function either as a permissive or a restrictive influence on synapse growth depends on a balance of FasII levels between the presynaptic and postsynaptic cells. Furthermore, we show that FasII and APPL form a biochemical complex *in vivo* and that the ability of FasII to promote new synapse formation requires an APPL-dependent transduction cascade. Finally, we show that dX11 interacts with APPL *in vivo* and is involved in APPL/FasII-dependent new synaptic bouton formation.

Role of APPL and FasII in promoting new synaptic bouton formation

During the development of the larval NMJ, as muscles continuously increase in size, synaptic efficacy is maintained in part by the formation of new synaptic boutons (Packard et al., 2003). In this process, FasII plays two fundamental roles: one of maintenance, as exemplified in the absence of FasII, when synaptic boutons begin to form but later retract, and a role in bouton proliferation (Schuster et al., 1996a). Although the role of FasII in synaptic maintenance might be related to its ability to mediate cell adhesion between the presynaptic and postsynaptic membranes, its ability to regulate budding mostly depends on genetic interactions with APPL: in the absence of APPL, a symmetric increase or decrease in FasII levels has no influence or even decreases bouton number. Although APPL is not absolutely required for synaptic growth, elimination of APPL results in significantly smaller arbors (Torroja et al., 1999).

We found that APPL was required for both FasII-dependent synaptic growth and for many physiological abnormalities accompanying NMJ structural defects. Although the bouton number decrease in *Appl* null mutants was correlated with a decreased amplitude of evoked synaptic responses, the bouton number increase in $fasII^{e76}$/+ was correlated with increased EJP amplitude. This increase was suppressed (to $Appl^{d}$ levels) by eliminating APPL in $fasII^{e76}$/+ mutants. In [FasII]-pre-post, however, the

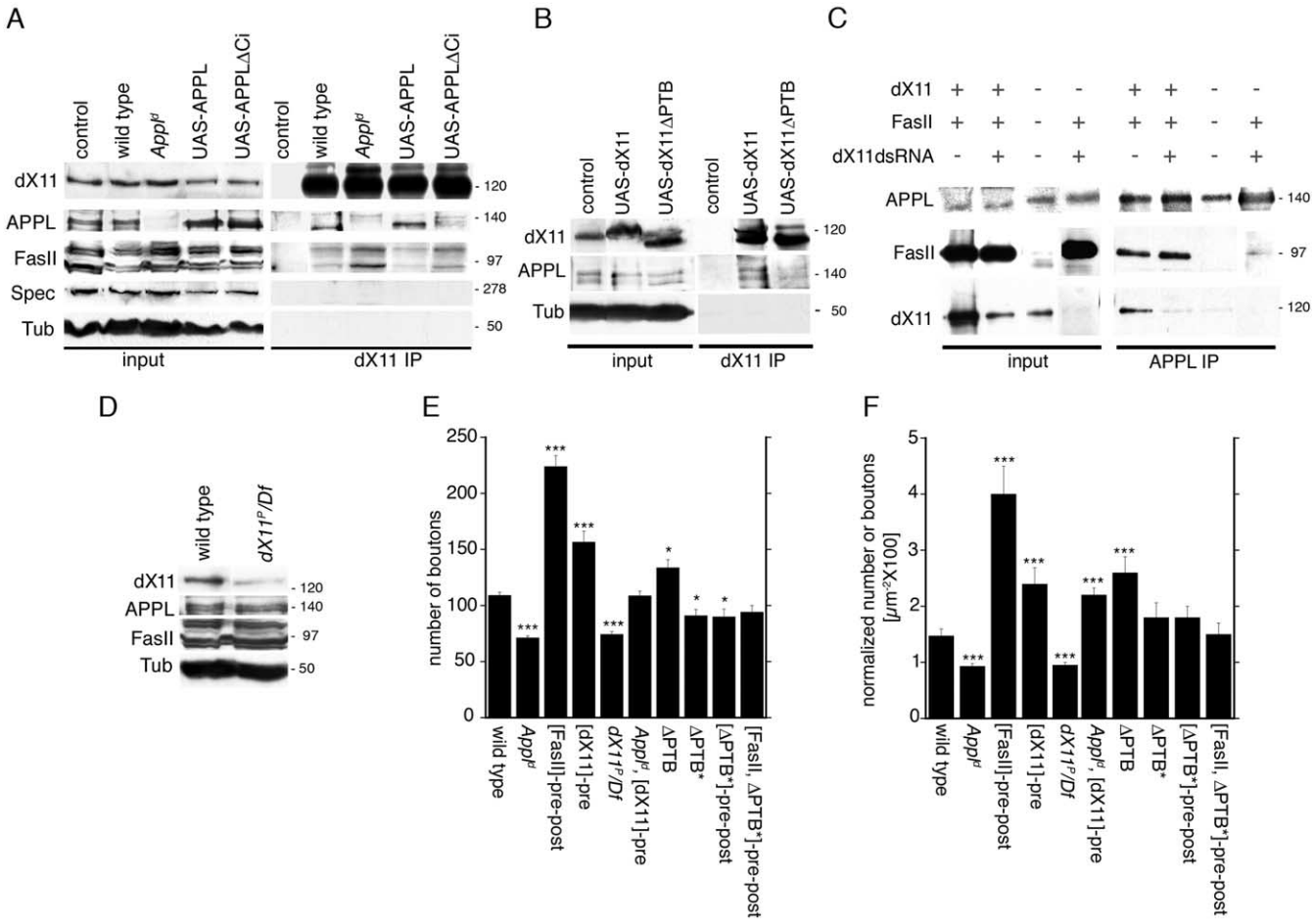

Figure 7. FasII stimulates NMJ expansion by a mechanism that requires both APPL and dX11, and dX11 exists in the APPL–FasII complex. ***A***, Antibodies against dX11 were used to immunoprecipitate dX11 from body-wall muscles of wild type, APPL gain- and loss-of-function mutants, and a strain expressing APPL but lacking the dX11-interacting domain (APPLΔCi). The blot was sequentially blotted with antibodies against dX11, APPL, FasII, spectrin (Spec), and tubulin (Tub). ***B***, Anti-dX11 antibody was used to immunoprecipitate dX11 from body-wall muscle extracts of larvae expressing a full-length dX11 and larvae expressing dX11 lacking the APPL interaction domain (dX11ΔPTB) and sequentially probed with antibodies against dX11, APPL, and tubulin. ***C***, Antibodies against APPL were used to immunoprecipitate APPL from *Drosophila* S2 cells expressing FasII and/or dX11. In some cases, cells were also treated with dX11 dsRNA. Blots were sequentially probed with antibodies against APPL, FasII, and dX11. ***D***, Western blots of body-wall muscle extracts from wild-type and $dX11^{P}/Df$ larvae probed with antibodies against dX11, APPL, FasII, and tubulin. ***E***, The histogram shows the total number of boutons at muscles 6 and 7 (abdominal segment 3) of third instar wild type, FasII, APPL, and dX11 genetic variants. ***F***, Bouton numbers have been normalized by muscle surface area. The number of samples quantified in ***E*** is as follows: wild type, $n = 95$; $Appl^{d}$, $n = 49$; [FasII]-pre-post, $n = 13$, [dX11]-pre, $n = 8$; $Appl^{d}$, [dX11]-pre, $n = 13$; [ΔPTB], $n = 14$; [ΔPTB]#, $n = 10$; [ΔPTB]-pre-post, $n = 8$. The number of samples quantified for ***F*** is as follows: wild type, $n = 30$; $Appl^{d}$, $n = 23$; [FasII]-pre-post, $n = 13$, [dX11]-pre, $n = 14$; $Appl^{d}$, [dX11]-pre, $n = 13$; [ΔPTB], $n = 14$; [ΔPTB]-pre-post, $n = 8$; $dX11^{P}/Df = 16$. $^{*}p < 0.05$; $^{***}p < 0.0001$. Error bars represent SEM.

dramatic increase in buds was correlated with an EJP amplitude decrease, possibly because these boutons were buds or immature boutons. Similarly, in [APPL]-pre, there was both an increase in buds and a decrease in EJP amplitude. Remarkably, as seen in the $fasII^{e76}$/+ mutants, the EJP phenotype is suppressed in the $Appl^{d}$ background (again, reaching $Appl^{d}$ levels). Thus, as in the morphological studies, many physiological abnormalities elicited by changing FasII levels depended on APPL. Interestingly, $Appl^{d}$ does mimic many electrophysiological phenotypes reported previously in $fasII^{e76}$ homozygotes, in that both show increased mEJP frequency, increased mEJP amplitude, and decreased bouton number (Stewart et al., 1996).

Activation of the synapse-promoting activity of APPL by FasII depended on simultaneous changes in the presynaptic and postsynaptic cell, whereas a unilateral change in FasII in either cell alone interfered with synapse formation. This may relate to the ability of FasII to establish *cis*- and *trans*-homophilic interactions and to the exclusive presynaptic expression of APPL (Luo et al., 1990).

FasII signaling through APPL

A genetic interaction between *Appl* and *fasII* was clearly demonstrated in our studies. We also demonstrated that both proteins form an endogenous complex at the NMJ and that this complex includes the APPL-binding protein dX11. In these interactions, we found that FasII could independently interact with both APPL and dX11. In the absence of APPL, an interaction between dX11 and FasII was maintained, whereas in the absence of dX11, interactions between APPL and FasII were preserved. Precisely how APPL and FasII proteins interact physically remains unclear. However, we found that, as was the case for APPL, the FasII intracellular domain was essential for the budding phenotype, suggesting that they may interact through their intracellular domains (Torroja et al., 1999). In the case of FasII and dX11, FasII contains a PDZ-binding motif, which interacts with PDZ1–PDZ2 domains of DLG (Thomas et al., 1997). It is possible that PDZ domains of dX11 are alternative FasII-interacting domains.

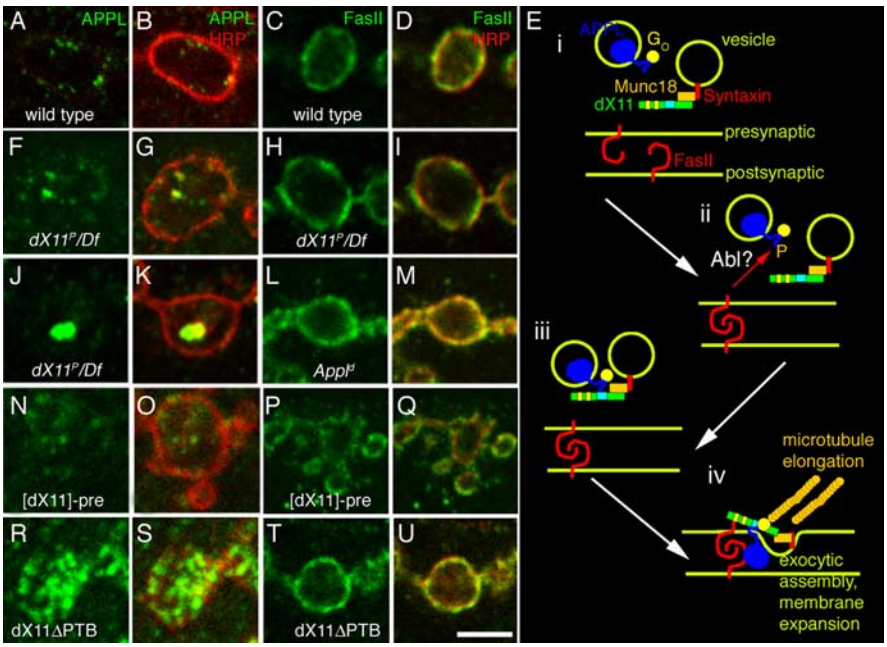

Figure 8. The localization of APPL at synaptic boutons is disrupted in *dX11* mutants and a model of likely interactions between FasII, dX11, and APPL during bouton budding. ***A–D***, ***F–U***, Single confocal slices of representative boutons stained with anti-APPL (***A***, ***F***, ***J***, ***N***, ***R***), anti-APPL and anti-HRP (***B***, ***G***, ***K***, ***O***, ***S***), anti-FasII (***C***, ***H***, ***L***, ***P***, ***T***), and anti-FasII and anti-HRP (***D***, ***I***, ***M***, ***Q***, ***U***), in wild type (***A–D***), $dX11^{P}/Df$ (***F–K***), $Appl^{d}$ (***L***, ***M***), [dX11]-pre (***N–Q***), and [dX11ΔPTB]-pre (***R–U***). Note that APPL is found at very low levels at the NMJ of wild type. In *dX11* mutants and in boutons from larvae overexpressing dX11ΔPTB, there are large internal accumulations of APPL. FasII staining changes little, if any, among the various dX11 specimens. Scale bar, 3.5 μm. ***E***, Diagram depicting likely interactions between FasII, APPL, and dX11 during bouton budding (see Discussion). ***Eii***, Homophilic binding between FasII molecules at opposing sides of the synapse triggers the activation of APPL, an event that may involve its phosphorylation by the tyrosine kinase Abl. ***Eiii***, APPL phosphorylation allows binding to the PTB domain of dX11, which brings or facilitates the insertion of APPL into the presynaptic membrane. dX11 also binds members of the exocytic machinery, thus bringing these components to the budding bouton. In addition, binding of APPL to FasII activates G_o protein, which modulates the microtubule cytoskeleton required for bud extension.

Role of dX11 in FasII–APPL-modulated synaptic growth

Our studies have identified a third member of the transduction cascade that promotes synaptic growth, dX11. First, dX11 was found in the same complex with APPL at the body-wall muscles, and the lack of the GYENPTY sequence of APPL or the PTB domain of dX11 suppressed or dramatically reduced this interaction, respectively. Second, a presynaptic increase of dX11 expression mimicked the effects of upregulating APPL. This effect was suppressed by deleting the PTB domain. Third, deleting the dX11–APPL interaction sequence in dX11 (dX11ΔPTB) mimicked the effect of deleting the APPL–dX11 interaction sequence (APPLΔCi) at the NMJ. Fourth, the effects of FasII gain-of-function in both the presynaptic and the postsynaptic cell were suppressed by expressing dX11ΔPTB, suggesting that the APPL and dX11 interaction is required for the effect of FasII. Finally, a hypomorphic *dX11* mutant mimicked the effects of eliminating APPL during NMJ expansion.

A variety of proteins that bind to the GYENPTY region of APP either increase APP translocation to the cell surface or alter the stabilization or cleavage of APP at the cell surface (Sabo et al., 1999; Taru et al., 2002). In particular, mammalian X11/Mint is highly expressed in neurons and interacts with the APP GYENPTY sequence through its single PTB domain (King et al., 2003). Neuronal X11 also associates directly with the exocytotic protein Munc-18, which in turn interacts with syntaxin1A (Biederer and Sudhof, 2000; Graham et al., 2004). In our studies, we found that deleting the APPL interaction domain in dX11 resulted in large accumulations of APPL within boutons, suggesting that dX11 may be involved in transporting or facilitating the insertion of APPL into the presynaptic membrane.

Several studies suggest that APPL behaves as a G_o-protein-coupled receptor (Okamoto et al., 1995; Brouillet et al., 1999). G_o has been shown to be involved in microtubule polymerization (Wang and Rasenick, 1991; Wu et al., 2001), suggesting that one of the actions of APPL during NMJ expansion might be to regulate the cytoskeleton. Recent studies show that microtubule dynamics at the *Drosophila* NMJ are essential for bud maturation and extension (Ruiz-Canada et al., 2004). Based on these known interactions, the following model for APPL and dX11 function can be proposed (Fig. 8*E*). *Trans*-homophilic interactions between FasII molecules localized at the presynaptic and postsynaptic cell activate the binding between the dX11 complex (containing exocytic molecules) and APPL (Fig. 8*Ei–Eiii*). dX11 then transports its partners to sites of FasII-mediated cell adhesion (Fig. 8*Eiv*). This results, on one hand, in the transport of the exocytic machinery and perhaps the addition of new membrane to sites of budding. In contrast, the insertion of APPL into the presynaptic membrane and its interactions with FasII activate G_o, resulting in the stimulation of microtubule polymerization, which is required for bud extension (Fig. 8*Eiv*).

The notion that FasII might function not only as a cell adhesion molecule but also as a signaling molecule is not without precedence (for review, see Packard et al., 2003). Indeed, the mammalian FasII homolog NCAM has been shown to initiate a signal transduction cascade after activation of both nonreceptor tyrosine kinases (nRTKs) and RTKs that may influence neurite outgrowth (Beggs et al., 1997). Interestingly, a genetic interaction between *fasII* and the nRTK Abelson tyrosine kinase gene (*Abl*) has been reported previously in flies (Garcia-Alonso et al., 1995), and, in mammals, activated Abl interacts directly with and phosphorylates the APP intracellular GYENPTY sequence (Zambrano et al., 2001; Perkinton et al., 2004). A variety of kinases are able to phosphorylate the APP cytoplasmic domain, resulting in regulation of APP metabolism and function (Aplin et al., 1996; Ando et al., 2001; Inomata et al., 2003; Standen et al., 2003). Phosphorylation of Thr668 of APP695 serves as a molecular switch that appears to regulate X11 binding to APP (Ando et al., 2001; Taru and Suzuki, 2004). Thus, phosphorylation of APPL could be the switch that leads to dX11 binding and subsequent translocation of APPL to the presynaptic membrane in the *Drosophila* NMJ.

APPL function and Alzheimer's disease

Our studies show that an asymmetric increase in FasII at the presynaptic cell interferes with normal synaptic bouton formation. This is characterized by formation of grossly abnormal boutons containing internal membrane structures with unusual APPL deposits and microtubule tangles surrounding these deposits. These internal APPL accumulations within the boutons

seem reminiscent of intraneuronal amyloid-β accumulation, which may precede extracellular amyloid plaque formation in Alzheimer's disease (D'Andrea et al., 2001; Glabe, 2001; Takahashi et al., 2002; Oddo et al., 2003). This phenomenon may provide additional clues toward a mechanism by which interference with normal APP function could lead to pathological events and subsequent symptoms of Alzheimer's disease.

In conclusion, we demonstrated via genetic analysis that APPL, FasII, and dX11 are involved in the same pathway that regulates synaptic expansion at the *Drosophila* NMJ. Altogether, these results suggest that beyond a role in cell adhesion, FasII-mediated signaling depends on a precise balance of its levels of expression at the presynaptic and postsynaptic cell and is likely to activate intracellular transduction pathways that control synapse structure.

References

Ando K, Iijima KI, Elliott JI, Kirino Y, Suzuki T (2001) Phosphorylation-dependent regulation of the interaction of amyloid precursor protein with Fe65 affects the production of beta-amyloid. J Biol Chem 276:40353–40361.

Aplin AE, Gibb GM, Jacobsen JS, Gallo JM, Anderton BH (1996) In vitro phosphorylation of the cytoplasmic domain of the amyloid precursor protein by glycogen synthase kinase-3beta. J Neurochem 67:699–707.

Bailey CH, Chen M, Keller F, Kandel ER (1992) Serotonin-mediated endocytosis of apCAM: an early step of learning-related synaptic growth in *Aplysia*. Science 256:645–649.

Bailey CH, Kaang BK, Chen M, Martin KC, Lim CS, Casadio A, Kandel ER (1997) Mutation in the phosphorylation sites of MAP kinase blocks learning-related internalization of apCAM in *Aplysia* sensory neurons. Neuron 18:913–924.

Beggs HE, Baragona SC, Hemperly JJ, Maness PF (1997) NCAM140 interacts with the focal adhesion kinase p125(fak) and the SRC-related tyrosine kinase p59(fyn). J Biol Chem 272:8310–8319.

Biederer T, Sudhof TC (2000) Mints as adaptors. Direct binding to neurexins and recruitment of munc18. J Biol Chem 275:39803–39806.

Biederer T, Sara Y, Mozhayeva M, Atasoy D, Liu X, Kavalali ET, Sudhof TC (2002) SynCAM, a synaptic adhesion molecule that drives synapse assembly. Science 297:1525–1531.

Borg JP, Ooi J, Levy E, Margolis B (1996) The phosphotyrosine interaction domains of X11 and FE65 bind to distinct sites on the YENPTY motif of amyloid precursor protein. Mol Cell Biol 16:6229–6241.

Brand AH, Perrimon N (1993) Targeted gene expression as a means of altering cell fates and generating dominant phenotypes. Development 118:401–415.

Brouillet E, Trembleau A, Galanaud D, Volovitch M, Bouillot C, Valenza C, Prochiantz A, Allinquant B (1999) The amyloid precursor protein interacts with G_o heterotrimeric protein within a cell compartment specialized in signal transduction. J Neurosci 19:1717–1727.

Budnik V, Zhong Y, Wu CF (1990) Morphological plasticity of motor axons in *Drosophila* mutants with altered excitability. J Neurosci 10:3754–3768.

Budnik V, Koh YH, Guan B, Hartmann B, Hough C, Woods D, Gorczyca M (1996) Regulation of synapse structure and function by the *Drosophila* tumor suppressor gene dlg. Neuron 17:627–640.

D'Andrea MR, Nagele RG, Wang HY, Peterson PA, Lee DH (2001) Evidence that neurones accumulating amyloid can undergo lysis to form amyloid plaques in Alzheimer's disease. Histopathology 38:120–134.

Davis GW, Goodman CS (1998) Synapse-specific control of synaptic efficacy at the terminals of a single neuron. Nature 392:82–86.

Davis GW, Schuster CM, Goodman CS (1997) Genetic analysis of the mechanisms controlling target selection: target-derived Fasciclin II regulates the pattern of synapse formation. Neuron 19:561–573.

Garcia-Alonso L, VanBerkum MF, Grenningloh G, Schuster C, Goodman CS (1995) Fasciclin II controls proneural gene expression in *Drosophila*. Proc Natl Acad Sci USA 92:10501–10505.

Glabe C (2001) Intracellular mechanisms of amyloid accumulation and pathogenesis in Alzheimer's disease. J Mol Neurosci 17:137–145.

Gorczyca M, Augart C, Budnik V (1993) Insulin-like receptor and insulin-like peptide are localized at neuromuscular junctions in *Drosophila*. J Neurosci 13:3692–3704.

Graham ME, Barclay JW, Burgoyne RD (2004) Syntaxin/Munc18 interactions in the late events during vesicle fusion and release in exocytosis. J Biol Chem 279:32751–32760.

Grenningloh G, Rehm EJ, Goodman CS (1991) Genetic analysis of growth cone guidance in *Drosophila*: fasciclin II functions as a neuronal recognition molecule. Cell 67:45–57.

Hase M, Yagi Y, Taru H, Tomita S, Sumioka A, Hori K, Miyamoto K, Sasamura T, Nakamura M, Matsuno K, Suzuki T (2002) Expression and characterization of the *Drosophila* X11-like/Mint protein during neural development. J Neurochem 81:1223–1232.

Hummel T, Krukkert K, Roos J, Davis G, Klambt C (2000) *Drosophila* Futsch/22C10 is a MAP1B-like protein required for dendritic and axonal development. Neuron 26:357–370.

Huntley GW (2002) Dynamic aspects of cadherin-mediated adhesion in synapse development and plasticity. Biol Cell 94:335–344.

Inomata H, Nakamura Y, Hayakawa A, Takata H, Suzuki T, Miyazawa K, Kitamura N (2003) A scaffold protein JIP-1b enhances amyloid precursor protein phosphorylation by JNK and its association with kinesin light chain 1. J Biol Chem 278:22946–22955.

Iqbal K, Alonso AC, Gong CX, Khatoon S, Pei JJ, Wang JZ, Grundke-Iqbal I (1998) Mechanisms of neurofibrillary degeneration and the formation of neurofibrillary tangles. J Neural Transm Suppl 53:169–180.

Jia XX, Gorczyca M, Budnik V (1993) Ultrastructure of neuromuscular junctions in *Drosophila*: comparison of wild type and mutants with increased excitability. J Neurobiol [Erratum (1994) 25:893–8955] 24:1025–1044.

Johansen J, Halpern ME, Johansen KM, Keshishian H (1989) Stereotypic morphology of glutamatergic synapses on identified muscle cells of *Drosophila* larvae. J Neurosci 9:710–725.

King GD, Turner RS (2004) Adaptor protein interactions: modulators of amyloid precursor protein metabolism and Alzheimer's disease risk? Exp Neurol 185:208–219.

King GD, Perez RG, Steinhilb ML, Gaut JR, Turner RS (2003) X11alpha modulates secretory and endocytic trafficking and metabolism of amyloid precursor protein: mutational analysis of the YENPTY sequence. Neuroscience 120:143–154.

Koh YH, Popova E, Thomas U, Griffith LC, Budnik V (1999) Regulation of DLG localization at synapses by CaMKII-dependent phosphorylation. Cell 98:353–363.

Koh YH, Ruiz-Canada C, Gorczyca M, Budnik V (2002) The Ras1-mitogen-activated protein kinase signal transduction pathway regulates synaptic plasticity through fasciclin II-mediated cell adhesion. J Neurosci 22:2496–2504.

Lai A, Gibson A, Hopkins CR, Trowbridge IS (1998) Signal-dependent trafficking of beta-amyloid precursor protein-transferrin receptor chimeras in madin-darby canine kidney cells. J Biol Chem 273:3732–3739.

Luo L, Tully T, White K (1992) Human amyloid precursor protein ameliorates behavioral deficit of flies deleted for Appl gene. Neuron 9:595–605.

Luo LQ, Martin-Morris LE, White K (1990) Identification, secretion, and neural expression of APPL, a *Drosophila* protein similar to human amyloid protein precursor. J Neurosci 10:3849–3861.

Luthl A, Laurent JP, Figurov A, Muller D, Schachner M (1994) Hippocampal long-term potentiation and neural cell adhesion molecules L1 and NCAM. Nature 372:777–779.

Mathew D, Popescu A, Budnik V (2003) *Drosophila* amphiphysin functions during synaptic Fasciclin II membrane cycling. J Neurosci 23:10710–10716.

Mayford M, Kandel ER (1999) Genetic approaches to memory storage. Trends Genet 15:463–470.

Muller D, Wang C, Skibo G, Toni N, Cremer H, Calaora V, Rougon G, Kiss JZ (1996) PSA-NCAM is required for activity-induced synaptic plasticity. Neuron 17:413–422.

Murase S, Schuman EM (1999) The role of cell adhesion molecules in synaptic plasticity and memory. Curr Opin Cell Biol 11:549–553.

Oddo S, Caccamo A, Kitazawa M, Tseng BP, LaFerla FM (2003) Amyloid deposition precedes tangle formation in a triple transgenic model of Alzheimer's disease. Neurobiol Aging 24:1063–1070.

Okamoto T, Takeda S, Murayama Y, Ogata E, Nishimoto I (1995) Ligand-dependent G protein coupling function of amyloid transmembrane precursor. J Biol Chem 270:4205–4208.

Packard M, Koo ES, Gorczyca M, Sharpe J, Cumberledge S, Budnik V (2002)

The *Drosophila* wnt, wingless, provides an essential signal for pre- and postsynaptic differentiation. Cell 111:319–330.

Packard M, Mathew D, Budnik V (2003) FASt remodeling of synapses in *Drosophila*. Curr Opin Neurobiol 13:527–534.

Panicker AK, Buhusi M, Thelen K, Maness PF (2003) Cellular signalling mechanisms of neural cell adhesion molecules. Front Biosci 8:d900–d911.

Paradis S, Sweeney ST, Davis GW (2001) Homeostatic control of presynaptic release is triggered by postsynaptic membrane depolarization. Neuron 30:737–749.

Perez RG, Soriano S, Hayes JD, Ostaszewski B, Xia W, Selkoe DJ, Chen X, Stokin GB, Koo EH (1999) Mutagenesis identifies new signals for beta-amyloid precursor protein endocytosis, turnover, and the generation of secreted fragments, including Abeta42. J Biol Chem 274:18851–18856.

Perkinton MS, Standen CL, Lau KF, Kesavapany S, Byers HL, Ward M, McLoughlin DM, Miller CC (2004) The c-Abl tyrosine kinase phosphorylates the Fe65 adaptor protein to stimulate Fe65/amyloid precursor protein nuclear signaling. J Biol Chem 279:22084–22091.

Roos J, Hummel T, Ng N, Klambt C, Davis GW (2000) *Drosophila* Futsch regulates synaptic microtubule organization and is necessary for synaptic growth. Neuron 26:371–382.

Ruiz-Canada C, Ashley J, Moeckel-Cole S, Drier E, Yin J, Budnik V (2004) New synaptic bouton formation is disrupted by misregulation of microtubule stability in aPKC mutants. Neuron 42:567–580.

Sabo SL, Lanier LM, Ikin AF, Khorkova O, Sahasrabudhe S, Greengard P, Buxbaum JD (1999) Regulation of beta-amyloid secretion by FE65, an amyloid protein precursor-binding protein. J Biol Chem 274:7952–7957.

Sastre M, Turner RS, Levy E (1998) X11 interaction with beta-amyloid precursor protein modulates its cellular stabilization and reduces amyloid beta-protein secretion. J Biol Chem 273:22351–22357.

Schmid RS, Graff RD, Schaller MD, Chen S, Schachner M, Hemperly JJ, Maness PF (1999) NCAM stimulates the Ras-MAPK pathway and CREB phosphorylation in neuronal cells. J Neurobiol 38:542–558.

Schuster CM, Davis GW, Fetter RD, Goodman CS (1996a) Genetic dissection of structural and functional components of synaptic plasticity. I. Fasciclin II controls synaptic stabilization and growth. Neuron 17:641–654.

Schuster CM, Davis GW, Fetter RD, Goodman CS (1996b) Genetic dissection of structural and functional components of synaptic plasticity. II. Fasciclin II controls presynaptic structural plasticity. Neuron 17:655–667.

Selkoe DJ, Podlisny MB (2002) Deciphering the genetic basis of Alzheimer's disease. Annu Rev Genomics Hum Genet 3:67–99.

Spillantini MG, Goedert M (1998) Tau protein pathology in neurodegenerative diseases. Trends Neurosci 21:428–433.

Spradling AC (1986) P-element-mediated transformation. In: *Drosophila*—a practical approach (Roberts DB, ed), pp 175–191. Oxford: IRL.

Standen CL, Perkinton MS, Byers HL, Kesavapany S, Lau KF, Ward M, McLoughlin D, Miller CC (2003) The neuronal adaptor protein Fe65 is phosphorylated by mitogen-activated protein kinase (ERK1/2). Mol Cell Neurosci 24:851–857.

Stewart BA, Atwood HL, Renger JJ, Wang J, Wu C-F (1994) *Drosophila* neuromuscular preparations in haemolymph-like physiological salines. J Comp Physiol [A] 175:179–191.

Stewart BA, Schuster CM, Goodman CS, Atwood HL (1996) Homeostasis of synaptic transmission in *Drosophila* with genetically altered nerve terminal morphology. J Neurosci 16:3877–3886.

Takahashi RH, Milner TA, Li F, Nam EE, Edgar MA, Yamaguchi H, Beal MF, Xu H, Greengard P, Gouras GK (2002) Intraneuronal Alzheimer abeta42 accumulates in multivesicular bodies and is associated with synaptic pathology. Am J Pathol 161:1869–1879.

Tang WJ (1993) Blot-affinity purification of antibodies. Methods Cell Biol 37:95–104.

Taru H, Suzuki T (2004) Facilitation of stress-induced phosphorylation of beta-amyloid precursor protein family members by X11-like/Mint2 protein. J Biol Chem 279:21628–21636.

Taru H, Kirino Y, Suzuki T (2002) Differential roles of JIP scaffold proteins in the modulation of amyloid precursor protein metabolism. J Biol Chem 277:27567–27574.

Thomas U, Kim E, Kuhlendahl S, Koh YH, Gundelfinger ED, Sheng M, Garner CC, Budnik V (1997) Synaptic clustering of the cell adhesion molecule fasciclin II by discs-large and its role in the regulation of presynaptic structure. Neuron 19:787–799.

Tomita S, Ozaki T, Taru H, Oguchi S, Takeda S, Yagi Y, Sakiyama S, Kirino Y, Suzuki T (1999) Interaction of a neuron-specific protein containing PDZ domains with Alzheimer's amyloid precursor protein. J Biol Chem 274:2243–2254.

Torroja L, Luo L, White K (1996) APPL, the *Drosophila* member of the APP-family, exhibits differential trafficking and processing in CNS neurons. J Neurosci 16:4638–4650.

Torroja L, Packard M, Gorczyca M, White K, Budnik V (1999) The *Drosophila* β-amyloid precursor protein homolog promotes synapse differentiation at the neuromuscular junction. J Neurosci 19:7793–7803.

Wang N, Rasenick MM (1991) Tubulin-G protein interactions involve microtubule polymerization domains. Biochemistry 30:10957–10965.

Welzl H, Stork O (2003) Cell adhesion molecules: key players in memory consolidation? News Physiol Sci 18:147–150.

Wu HC, Chiu CY, Huang PH, Lin CT (2001) The association of heterotrimeric GTP-binding protein (Go) with microtubules. J Biomed Sci 8:349–358.

Zambrano N, Bruni P, Minopoli G, Mosca R, Molino D, Russo C, Schettini G, Sudol M, Russo T (2001) The beta-amyloid precursor protein APP is tyrosine-phosphorylated in cells expressing a constitutively active form of the Abl protoncogene. J Biol Chem 276:19787–19792.

Zhang Z, Lee CH, Mandiyan V, Borg JP, Margolis B, Schlessinger J, Kuriyan J (1997) Sequence-specific recognition of the internalization motif of the Alzheimer's amyloid precursor protein by the X11 PTB domain. EMBO J 16:6141–6150.

Zito K, Parnas D, Fetter RD, Isacoff EY, Goodman CS (1999) Watching a synapse grow: noninvasive confocal imaging of synaptic growth in *Drosophila*. Neuron 22:719–729.